Optimal Design of Heating Elements Sheathed with INCOLOY Superalloy 800

AUREL RĂDUȚĂ
aurel.raduta@mec.upt.ro

MIRCEA NICOARĂ
mircea.nicoara@mec.upt.ro

LAURENȚIU ROLAND CUCURUZ
roland.cucuruz@mec.upt.ro

COSMIN LOCOVEI
cosmin.locovei@mec.upt.ro
Department of Materials and Manufacturing Engineering,
POLITEHNICA University of Timişoara
Bd. M. Viteazul 1, 300222 Timişoara
ROMANIA

Abstract: - Electric heating has become in recent years the first choice for both industrial and household applications, since reduction of carbon dioxide emissions represents a major concern, and has caused replacement of solutions based on burning of gas or oil. Considering the importance of low energy consumption and increased functional safety, significant efforts have been made for design optimization. Microstructural analysis has determined that most of failures reported during exploitation and maintenance of electric heaters for production of hot water are caused by overheating of metallic components, although existing components are usually fabricated from heat resistant steels or super-alloys such as INCOLOY 800. Therefore constructive optimization has been based of an analysis of temperature distribution in heated water and on surface of heating element, using the finite elements, for both classical solutions, which are mostly based on empirical experience, and some new technical solutions that have been proposed to improve the existing design experience. The newly optimized solutions are based on new forms of heating elements, as well as different positions for water inlet or outlet. Simulations of temperature distributions indicate that optimized shapes of heating element are likely to improve both heating efficiency and reduce occurrence of failures.

Key-Words: - INCOLOY 800, Heat transfer, Pitting corrosion, Fluid flow, Electric heating, Finite elements

1 Introduction

Latest concerns for reducing of greenhouse gas emissions, considered the main reason responsible for anthropogenic global warming have boosted up both technical and managerial efforts of industrial companies worldwide. If industrial and household heating is concerned there are some evident directions to eliminate direct carbon dioxide emissions on which technical research and development are focused:

- Replacement of heating technologies based on burning of fossil fuel with different methods of electric heating;
- Optimization of heating efficiency based on electric energy, in order to reduce losses and specific consumptions;

It is well known that production of electric energy is still based in many cases on burning of fossil sources (coal, gas, oil), and is also producing carbon dioxide emissions.

However it may be considered that fuel burning is more efficient in power plants, which could more easily adopt environment-friendly technologies. On the other hand consumption of electric energy will virtually benefit from all improvements implemented in electricity production, and their positive effects will propagate to all industrial processes that use electric energy instead of burning fossil fuel.

Although electric energy has been considered for many years to be cheap and inexhaustible, increased energy

prices and environmental consciousness have triggered considerable efforts to improve product design, for better performances and durability, especially when large scale production is involved.

2 Description of instant water heater

2.1 General characteristics

A typical electric heater, which is subject to optimization, is composed of a stainless steel container (figure 1) and an electric heater (figure 2). The water is provided by mean of an inlet orifice, heated during the contact with the surface of heating element, and expulsed through the outlet orifice. The heater is calculated to heat a quantity of 1 liter of water/minute, i.e. 0,017 liters/second or 60 liters of water every hour. The average temperature of the heated water should be between 60 and 70°C.

Fig. 1. General appearance of an electric industrial heater for instant heating of water.

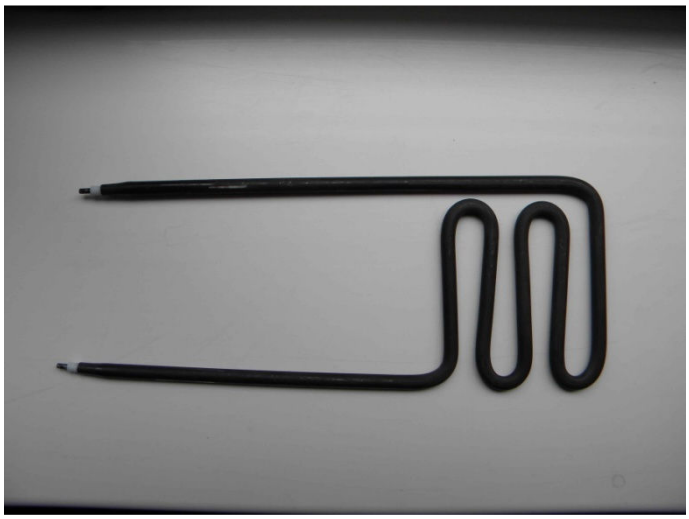

Fig. 2. Configuration of heating element.

The heater is provided with an electric heating element, which supplies a net heating power of 3500 W.
The main parameters of heating regime are presented in Table 1.

Table 1. Parameters of water heating.

Parameter	Value
Water mass flow [kg/s]	0,017
Voltage on heating element [V]	240
Thermal power [W]	3500
Max. fluid temperature range [°C]	60±3
Min. fluid temperature range [°C]	70±3
Max. temperature on heating element [°C]	900

2.2 Electric heating element

Typical heating element, as seen in figure 3, consists of a helical Ni-based resistive wire (1), an isolation of magnesium oxide powder (2) and an exterior protection tube of INCOLOY 800 (3).

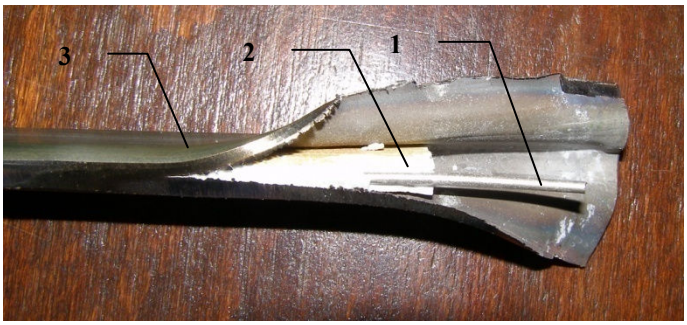

Fig. 3. Composition of the heating element: 1-resistive wire, 2 – isolating powder, 3 – protection sheath.

INCOLOY 800 is a Ni-Cr-Fe alloy that represents the best alternative for the 300 series stainless steels when improved performance or strength at temperature is required. Among the most important applications that use INCOLOY 800 are heat treating equipment and fixtures, heating-element sheathing, heat exchangers, process piping, nuclear steam-generator tubing etc.
INCOLOY 800 is used for corrosion resistance, heat resistance, strength, and stability for service up to 816° C (1500°F). One remarkable attribute of this alloy is the fact that it also offers general corrosion resistance to many aqueous media. Thanks to its content of nickel, INCOLOY 800 resists stress corrosion cracking. At elevated temperatures it offers resistance to oxidation, carburization, and sulfidation along with rupture and creep strength.
The main reason for excellent behavior at high temperature could be explained by a very important feature of this alloy, which maintains a stable, austenitic structure during prolonged exposure to high temperatures.

In applications requiring greater resistance to stress rupture and creep, especially at temperatures above 816°C, INCOLOY alloys 800H and 800HT are used.
Typical chemical composition of INCOLOY alloys 800, 800H, and 800HT are presented in Table 2.

Table 2. Compositions for INCOLOY alloys

Element	Content [%]		
	Alloy 800	Alloy 800H	Alloy 800HT
Nickel	30.0-35.0	30.0-35.0	30.0-35.0
Chromium	19.0-23.0	19.0-23.0	19.0-23.0
Iron	39.5 min.	39.5 min.	39.5 min.
Carbon	0.10 max.	0.05-0.10	0.06-0.10
Aluminum	0.15-0.60	0.15-0.60	0.25-0.60
Titanium	0.15-0.60	0.15-0.60	0.25-0.60
Aluminum + Titanium	0.30-1.20	0.30-1.20	0.85-1.20

Austenitic structure is also favorable for processing by mean of plastic deformation, machining, welding etc.

2.3 Analysis of failure cases

A significant number of failure cases have been reported in relation with the electric heating element. In spite of use of Incoloy sheathing both exposure to high temperature and contact with hot water seem to be responsible for early breakdown of the electric heaters.

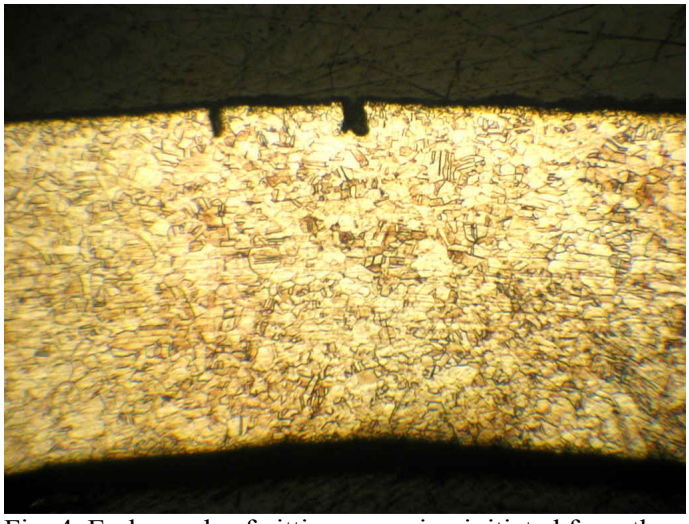

Fig. 4. Early seeds of pitting corrosion initiated from the exterior surface of the tube, OM (optical magnification) 100x, etched.

Early failure of Incoloy sheath appears in relation with the fabrication technology. A typical fabrication route of the sheathing tube consists of following operations:
- Cutting in narrow strips of the Incoloy sheets;
- Plastic deformation to form the tube shape;
- Tungsten inert gas (TIG) welding on the generator of the formed tube;
- Cutting off the tube to needed length.

Subsequently, resisting wire and powder of magnesium oxide are introduced into the tube, both ends are sealed, and finally the tube is shaped by plastic deformation.
An analysis of numerous failure cases, which occur during exploitation revealed two major causes of defect, both affecting the sheathing tube:
- Pitting corrosion that happens almost exclusively on the exterior face of the thin tube, which is in continuous contact with the boiling water, and
- Stress corrosion, which has been reported to initiate on both exterior and interior faces of the tube, but seems to be more frequent on the interior side.

Typical microstructural appearances of pitting and stress corrosion of the sheath are presented in figure 4 and figure 5, respectively.

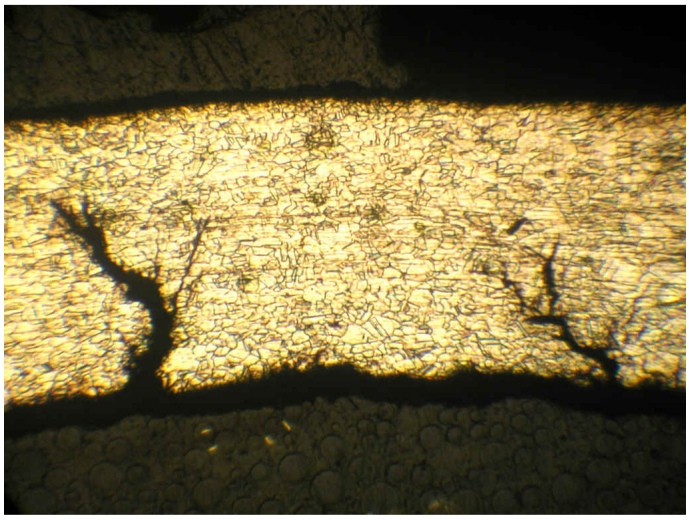

Fig. 5. Stress corrosion initiated from the interior surface of the tube OM 100x, etched.

Microstructural investigations have generally correlated stress corrosion with structural faults, such as increased grain size, aligned precipitated phases, excessive plastic deformation ratio, and other, usually related with fabrication non-conformities, and rarely caused by exploitation conditions.
On the contrary, pitting corrosions can be connected in many cases with overheating, when material surface is in contact with water, under the effect of significant proportion of halogens, possible chloride. This hypothesis could be enhanced by localization of pitting corrosion almost exclusively on the exterior surface of the sheath.
Failure of the heating element by pitting corrosion has an evolutive development. Initially only isolated points on the surface are affected, as seen on figure 6.

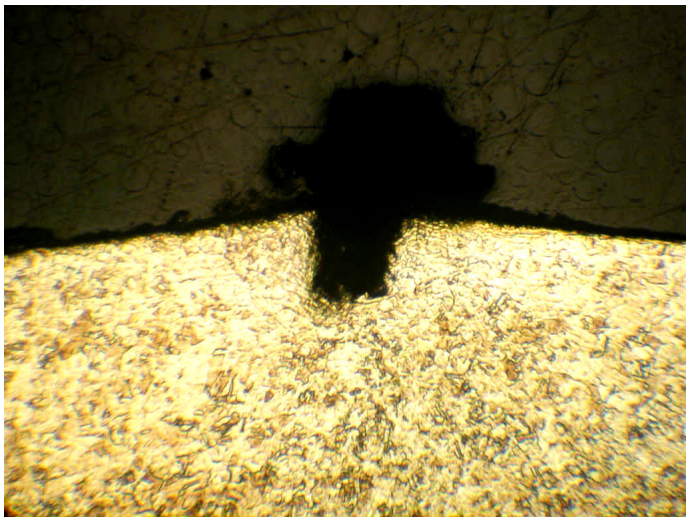

Fig. 6. Initial surface zone of pitting corrosion, OM 100x, etched.

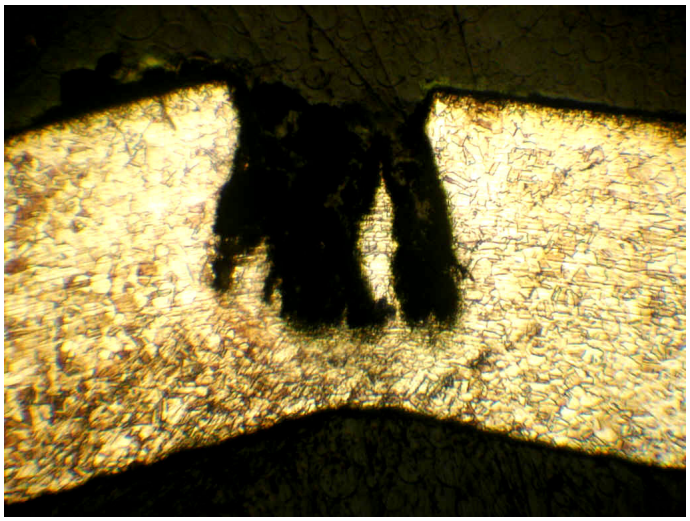

Fig. 7. Further evolution of corrosion cavity, OM 100x, etched.

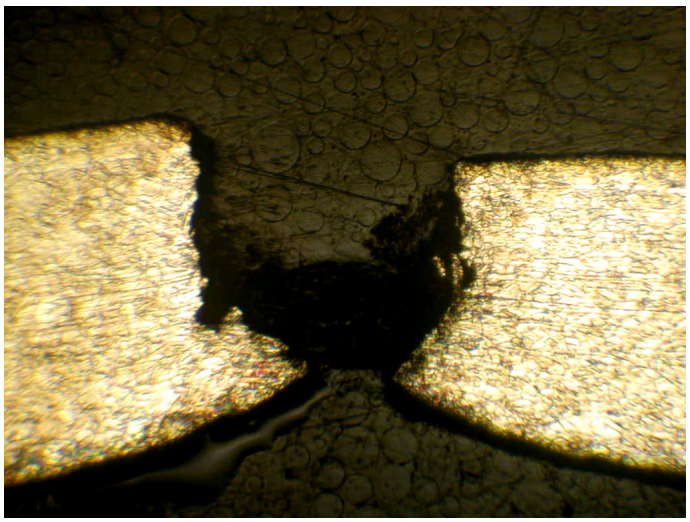

Fig 8. Final breakdown of the sheath, OM 100x, etched.

Continuous exposure to aqueous media and high temperature deepens the cavity, which affects more and more the thin wall of the tube (figure 7).
Finally most of wall section is corroded, the sheath brakes, and the heating element is out of service, with considerable damage involved (figure 8).
Significantly, among the considerable number of broken sheath, both inter-crystalline and trans- crystalline breaking mechanisms could be evidenced (figure 9 and 10).

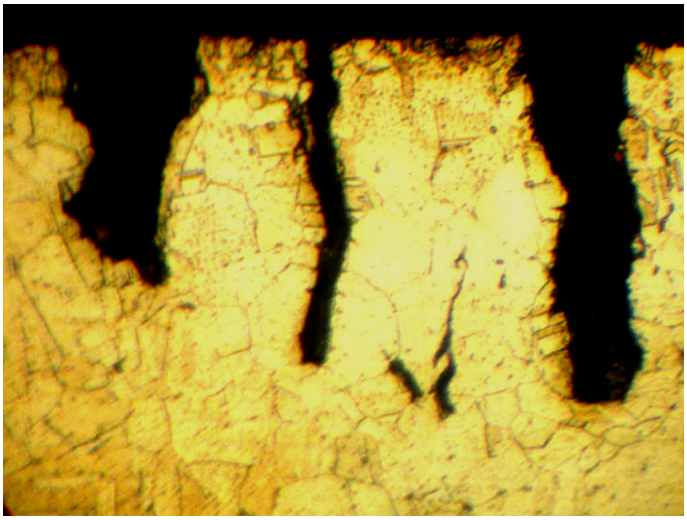

Fig. 9. Trans-crystalline breaking of the sheath wall, OM 500x, etched.

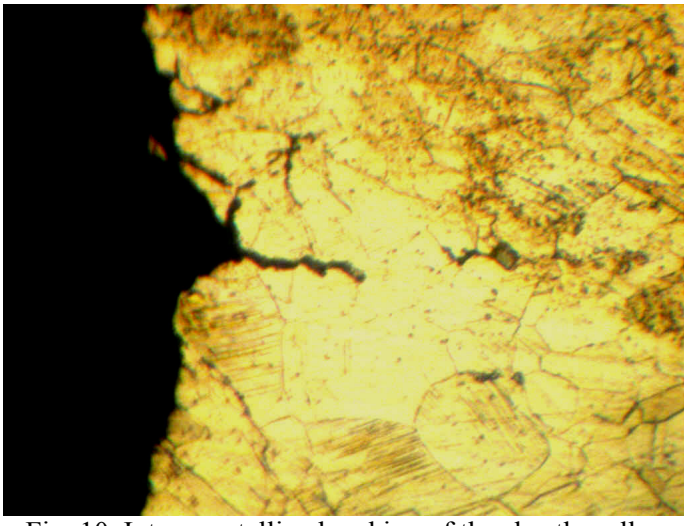

Fig. 10. Inter-crystalline breaking of the sheath wall, OM 500x, etched.

The incidence of both breaking mechanism suggests that failure causes are merely exterior to material, such as corrosion environment or temperature level, and not related with a specific material defect or non-homogeneity.

This last conclusion, corroborating with the predominance of pitting corrosion among the failure cases that have been reported during a long period of service, suggests that overheating of sheath on exterior surface could be a systematic cause of failure in service for the heating elements.
Therefore it has been decided that a detailed analysis of construction and design of heating element, with an emphasis on the heat transfer conditions, should be pursued in order to improve both efficiency and safety.

3 Analysis conditions

Considering the relatively complex configuration of heater, and the possible complicated flowing trajectories, it was decided an analysis on a three-dimensional model, which is considering both heat transfer and flowing of heated fluid. The simplified solid analyzed using the Flow Simulation software is presented in figure 11.

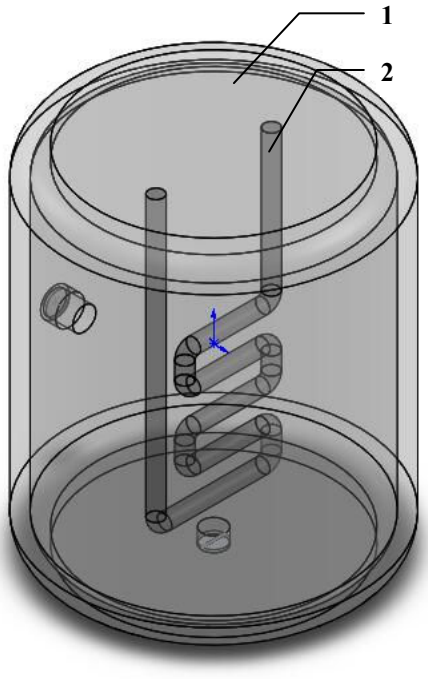

Fig. 11. General appearance of the three-dimensional model: 1 - container; 2 - heating element.

The study has considered the steady state condition for system, having the following thermal loads:
- The only energy input is provided by the heating element, which is supplying a constant thermal power produced through resistive transformation of electric energy E_{el};
- The main output is represented by the energy absorbed by forced convection E_w from the heating element by the constant flowing rate of water circulating through the stainless steel container;
- A secondary output of energy E_{am} is taken by the ambient. The heat is transferred by forced convection from the heated water to the interior surface of the steel container. The heat is traversing by conduction through container wall and is transfer by mean of natural convection to the ambient air.
The equilibrium equation could be written as:

$$E_{el} = E_w + E_{am} \qquad (1)$$

Figure 12 represents a schematic representation of energy balance.

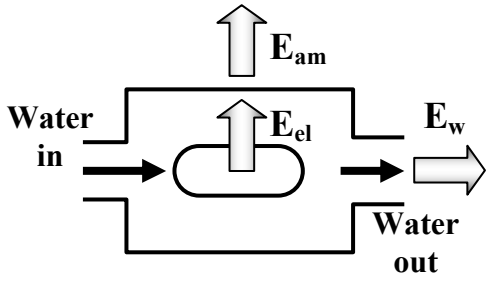

Fig. 12. Energy balance of the steady state system.

Heat transfer for water heating represents a complex case, involving convection and conduction. Electric heating element is converting electric energy into heat. For simplicity the surface of the heating element is considered to produce the entire thermal power, so the conduction effect from resistive wire to the heater sheath, through magnesium oxide powder is neglected.

3.1 Forced convection of external flow

Water heating in contact with metallic sheath could be represented as forced-convection expressed by external-flow problem. An external source causes the fluid to move past the curved surface of heater sheath. The rate of heat transfer could be determined by Newton's law of cooling:

$$q = h_{c,ext}(T_w - T_\infty) \qquad (2)$$

Where q is the heat flux, $h_{c,ext}$ represents the convection coefficient for external flow and the $(T_w\text{-}T_\infty)$ is the temperature difference between the fluid and solid surface, so that the heat transfer takes place.
Convection coefficient $h_{c,ext}$ has a very complex dependence on several variables, showed in relation (3)

and can be calculated locally by numerical methods, which allows determining the amount of energy transferred:

$$h_{c,ext}=f(\rho, V, x, \mu, c_p, \Delta T, k_f) \quad (3)$$

Symbols in relation (3) have the following significance:
- ρ = fluid density;
- V = local fluid velocity;
- x = a characteristic dimension that could be the distance from a leading edge, which influences fluid flowing cross section;
- μ = the dynamic viscosity of the fluid;
- c_p = the specific heat of the fluid;
- ΔT = temperature difference between wall and fluid;
- k_f = the thermal conductivity of the fluid;

Following relation can be obtained by performing a dimension analysis on equation (3):

$$\frac{h_{c,ext}x}{k_f} = f\left(\frac{\rho V x}{\mu}, \frac{c_p \mu}{k_f}, \frac{V^2}{c_p \Delta T}\right) \quad (4)$$

Dimensionless group in above equation have traditionally specific names:
- Nusselt number, generally interpreted as convection heat transfer:

$$Nu_x = \frac{h_{c,ext}x}{k_f} \quad (5)$$

- Reynolds number, which usually expresses viscous forces or inertia for a fluid:

$$Re_x = \frac{\rho V x}{\mu} \quad (6)$$

Reynolds number is an important criterion for determining whether a film of fluid is flowing laminar or turbulent, usually values below 1800 denoting a laminar flow.
- Prandtl number, which can be interpreted as kinematic viscosity for a fluid:

$$Pr = \frac{c_p \mu}{k_f} \quad (7)$$

For example Prandtl number of water has an important variation with temperature, from Pr = 7,02 at 20°C to 2,22 at 80°C
- Eckert number, expressing kinetic energy of flow:

$$Ec = \frac{V^2}{c_p \Delta T} \quad (8)$$

Equation (3) can be rewritten as (9), which is very useful for dimensional analysis of forced convection:

$$Nu_x = f(Re_x, Pr, Ec) \quad (9)$$

Dimensional analysis allows uncomplicated numerical calculation assisted by computer, as well as integration of experimental values.

3.2 Forced convection of internal flow

Rate of heat transfer between fluid and interior surface of the container is represented by forced-convection expressed by internal flow problem, and the relation is similar as for external flow (relation 2):

$$q = h_{c,int}(T_w - T_\infty) \quad (10)$$

Complex relationship of convection coefficient for internal flow with different factors is represented in equation (11)

$$h_{c,int}=f(\rho, V, D, \mu, c_p, \Delta T, k_f) \quad (11)$$

The only difference from relation (3) is that internal flow requires characteristic dimension *D* of the conduit cross-section, often referred as hydraulic diameter, instead distance *x* from leading edge.
Similarly with external flow, dimension analysis of equation (11) will result in following relation:

$$\frac{h_{c,int}D}{k_f} = f\left(\frac{\rho V D}{\mu}, \frac{c_p \mu}{k_f}, \frac{V^2}{c_p \Delta T}\right) \quad (12)$$

Dimensionless groups will become:
- Nusselt number:

$$Nu_D = \frac{h_{c,ext}D}{k_f} \quad (13)$$

- Reynolds number:

$$Re_D = \frac{\rho V D}{\mu} \quad (14)$$

- Prandtl number:

$$Pr = \frac{c_p \mu}{k_f} = \frac{\nu}{\alpha} \quad (15)$$

where ν represents the kinematic viscosity of fluid.
- Eckert number:

$$Ec = \frac{V^2}{c_p \Delta T} \quad (16)$$

Equation (12) can be rewritten as:

$$Nu_D = f(Re_D, Pr, Ec) \quad (17)$$

3.3 Natural convection

Energy losses from the steel container to ambient are facilitated by natural convection of ambient air in contact with warmer surfaces, plate-shaped for the frontal surfaces of container, and cylindrical for the lateral side.

As fluid near the warmed surface begins to increase in temperature, local fluid density decreases. The buoyant force causes the less dense fluid to rise, and cooler fluid is brought into contact with the surface. Therefore fluid-motion and heat-transfer effects are intimately related. For the general natural-convection problem the rate of heat transfer is governed by following relation:

$$q = h_{c,nat}(T_\infty - T_{air}) \quad (18)$$

In relation (18) $h_{c,nat}$ is the coefficient of natural convection and difference T_∞-T_{air} is the temperature difference between warm surfaces and ambient air.

Calculation of natural convection coefficient is based on the following relation:

$$h_{c,nat}=f(\rho, V, L, \mu, c_p, \Delta T, k_f, \beta) \quad (19)$$

Influence factors have the same significance as in relations (3) and (11). Additionally L is the characteristic length and β is the volumetric expansion coefficient of air.

Dimension analysis will give the following relation:

$$\frac{h_{c,nat}L}{k_f} = f\left(\frac{\rho VL}{\mu}, \frac{c_p\mu}{k_f}, \frac{\rho^2 g\beta\Delta TL^3}{\mu^2}, \frac{V^2}{c_p\Delta T}\right) \quad (20)$$

In equation (20) g is the gravitational acceleration, and the group containing the volumetric expansion coefficient is called the Grashof number:

$$Gr = \frac{\rho^2 g\beta\Delta TL^3}{\mu^2} = \frac{\beta\Delta TL^3}{\nu^2} \quad (21)$$

The Grashof number is considered for natural-convection problems where volumetric expansion coefficient β is significant, which is also the case of ambient air.

Other dimensionless groups that are used for natural convection are:

- Rayleigh number:

$$Ra = (Gr)(Pr) == \frac{g\beta\Delta TL^3}{\nu^2}\frac{\nu}{\alpha} = \frac{g\beta\Delta TL^3}{\nu\alpha} \quad (22)$$

- Stanton number:

$$St = \frac{Nu}{(Re)(\mathrm{Pr})} = \frac{h_{c,nat}L}{k_f}\frac{\nu}{VL}\frac{\alpha}{\nu} = \frac{h_{c,nat}L}{k_f}\frac{\nu}{VL}\frac{\alpha}{\nu}\frac{c_p\rho}{c_p\rho} =$$

$$St = \frac{h_{c,nat}}{\rho c_p V} \quad (23)$$

Finally, equation (20) can be rewritten:

$$Nu_L = f(Re, Pr, Gr_L, Ec) \quad (24)$$

3.4 Heat conduction in solid

The heat produced electrically by heating element is transferred by mean of forced convection to the flowing water, which transfers a certain proportion of that heat quantity, also by mean of forced convection to the interior surface of the steel container.

Calculation of heat transfer by mean of conduction, trough the wall of steel container is based on the Fourier's law of heat conduction, presented as relation (25):

$$\frac{q_x}{A} = k\frac{T_2 - T_1}{L} \quad (25)$$

In above relation the following annotations have been used:

- q_x is the heat flow in a certain direction;
- A is the area normal to the heat flow direction, and
- T_2-T_1 is the difference of temperature between 2 points on that particular direction, separated by a distance L.

Coefficient k is the thermal conductivity of the stainless steel used to fabricate the container.

The most importance boundary conditions applied to the model are:

- Calculation model is limited to the exterior limits of the container, and only the interior flowing of the fluid is simulated, both for laminar and turbulent flowing;
- Water inlet is constrained to a mass flow rate of 0,017 kg/s;
- Water outlet is constrained by a static pressure of 101325 Pa, corresponding to normal atmospheric pressure;
- Heat conduction in solids is considered, specifically the values for austenitic stainless steel AISI 304, used for fabrication of steel container, although the wall thickness is relatively small;
- Natural convection in air on the exterior of container is considered at 20 W/m^2 °C;

Heating power of 3500 W is considered uniformly distributed on the surface of the sheath of heating element.

The classic design has been evaluated to be satisfactory in terms of heating capacity and dimensions.

However maintenance information suggests relatively frequent failure of heating elements, probably as consequence of overheating. There are also some doubts related with the thermal uniformity of the outcoming water.

Since configuration of the heater is based on company experience and good practice, numerical analysis could give precious information for higher efficiency.

4 Analysis of flowing and heat transfer

Design optimization is based on simulation of fluid flowing inside container and heat transfer between heating element and fluid.

A number of 4 different cases that cover practically all possibilities of use for the heater have been considered, as follows:

1. The plane of heating element is perpendicular with the lateral orifice (as presented by figure 11), which represents the water inlet; water outlet is on the bottom of container (case no. 1);

This case also represents the actual construction, which is presently used for large scale fabrication of heaters;

2. Same orientation of the plane of heating element, but water inlet is on the bottom and outlet is on the lateral (case no. 2);
3. The plane of heating element is parallel with the axis of lateral orifice, which is also the water inlet; water outlet is on the bottom (case no. 3);
4. Same orientation of heating element, with water inlet on the bottom and outlet in lateral (case no. 4);

The thermal fields of the water content have been determined in two different vertical sections. These distributions for case no. 1 are presented together with surface temperature distribution on the heating element in figure 12.

There is also of practical interest to determine temperature variation along the diameter of the outlet orifice, since this distribution is actually determining the output of the heater. This particular variation is presented in figure 13.

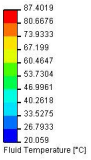

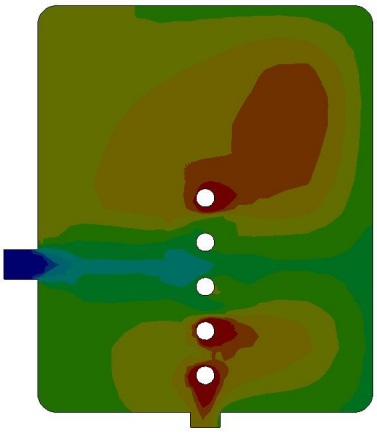

(a) fluid temperature through front vertical section.

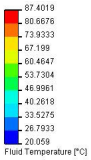

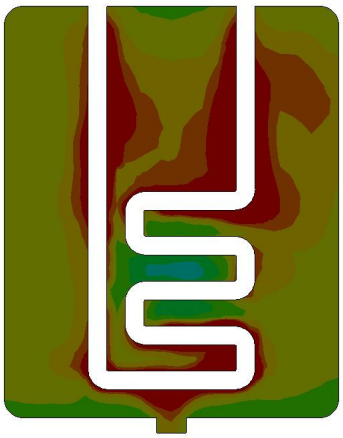

(b) fluid temperature through lateral vertical section.

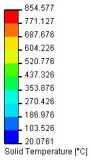

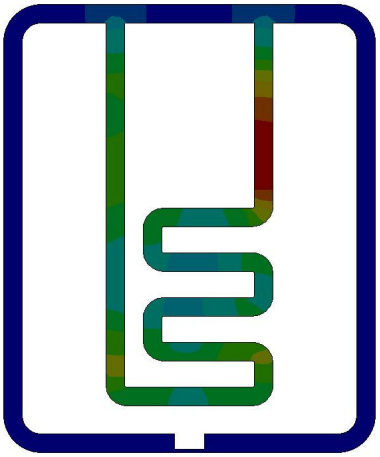

(c) solid temperature through lateral vertical section.

Fig. 12. Distribution of temperature for case no.1

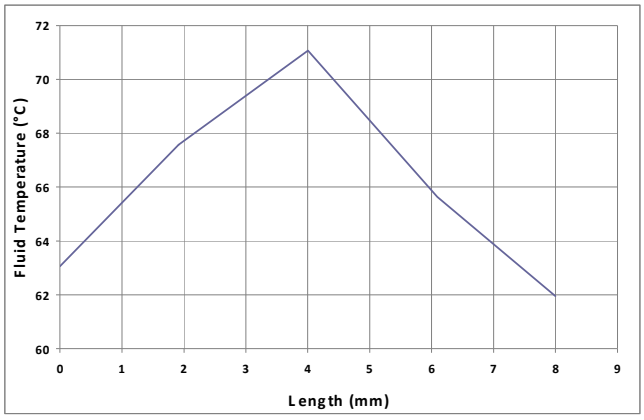

Fig. 13. Variation of water temperature on the outlet for case no.1.

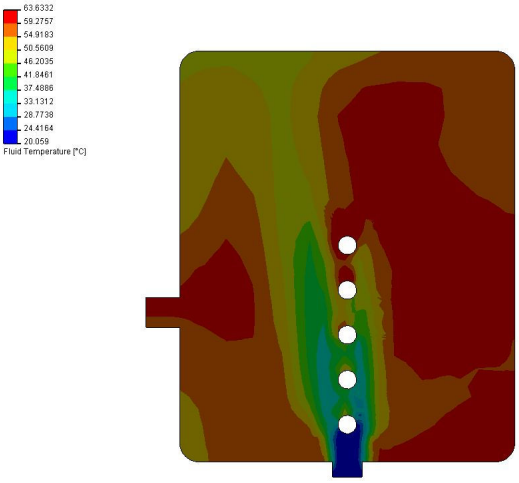

(a) fluid temperature through front vertical section.

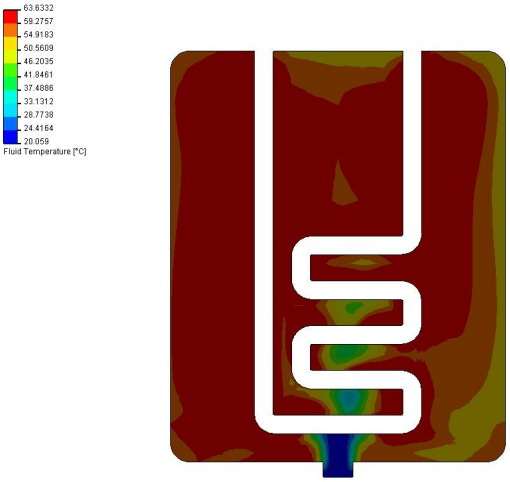

(b) fluid temperature through lateral vertical section.

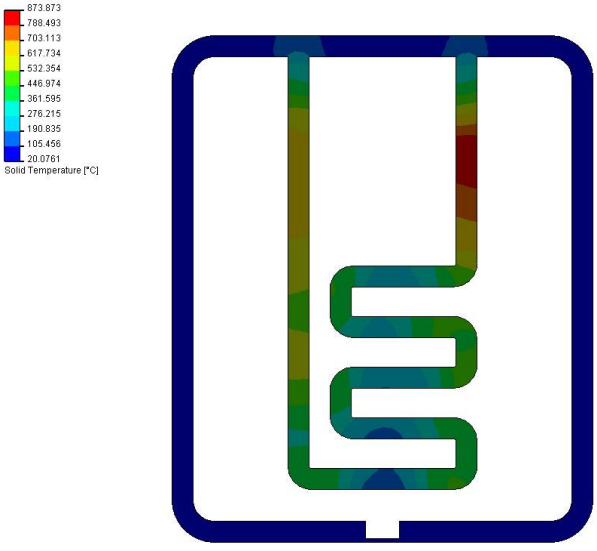

(c) solid temperature through lateral vertical section.

Fig. 14. Distribution of temperature for case no.2

The result of water heating could be considered satisfactory, since fluid leaves container at a temperature that comply with the generally requirements, i.e. between 60 and 70°C. However water has the highest temperature inside the container and not at exit, which does not assure optimum efficiency.

On the other hand, heating element is not symmetrically loaded, and has an area where temperature is close to 900°C, which is the upper limit of working range, and could be responsible for early failure and reduced durability, as reported in some cases.

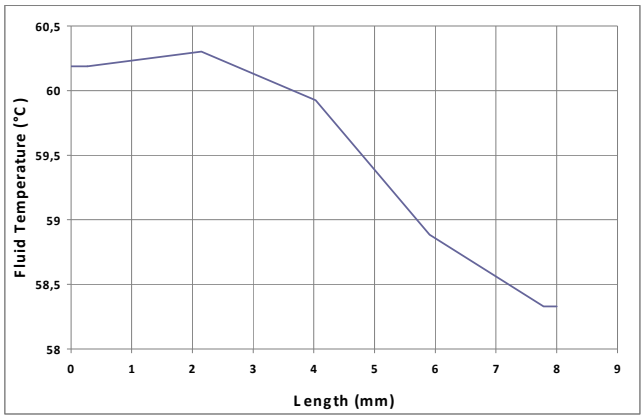

Fig. 15. Variation of water temperature on the outlet for case no.2.

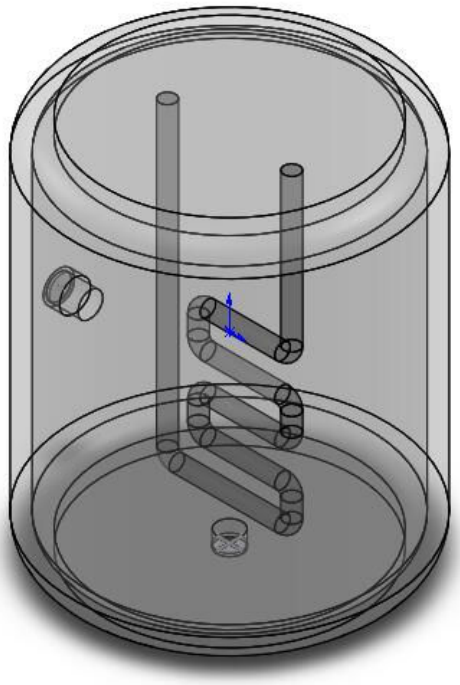

Fig. 16. General appearance of the three-dimensional model for case no. 3 and 4.

If bottom orifice is used as water inlet (figure 14), as occasionally could happened, if an incorrect assembly is made, the maximum fluid temperature is lower, and water temperature at exit is toward the lower limit, although the gradient is smaller (figure 15).
The maximum temperature on the heating element is even closer to the 900°C limit, which also endangers durability.

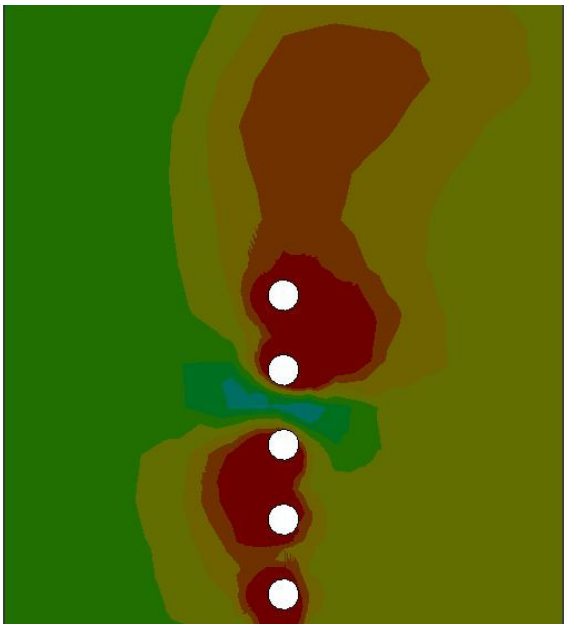

(a) fluid temperature through front vertical section.

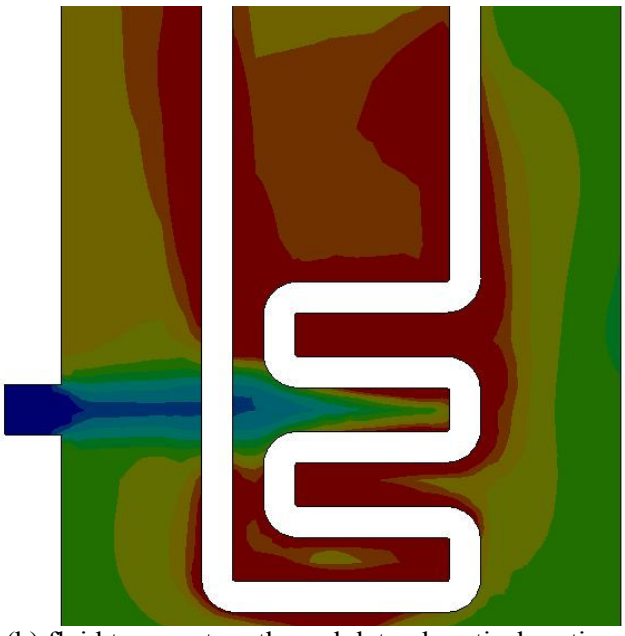

(b) fluid temperature through lateral vertical section.

Modifying the position of heating element relative to the lateral orifice of container, is also changing conditions for fluid flowing and heat transfer (figure 16).

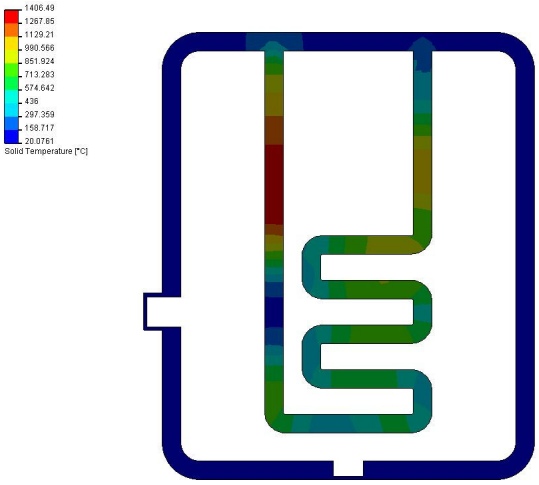

(c) solid temperature through lateral vertical section.

Fig. 17. Distribution of temperature for case no.3

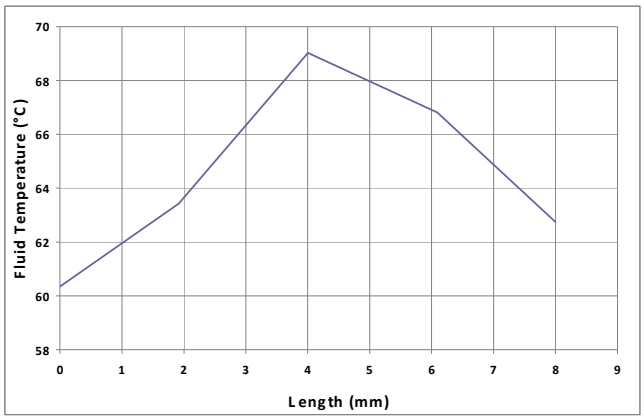

Fig. 18. Variation of water temperature on the outlet for case no.3.

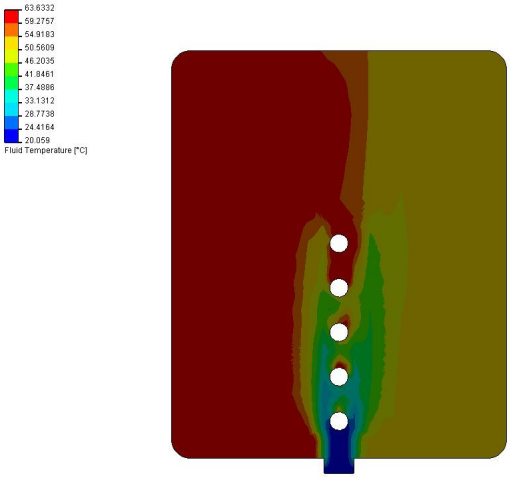

(a) fluid temperature through front vertical section.

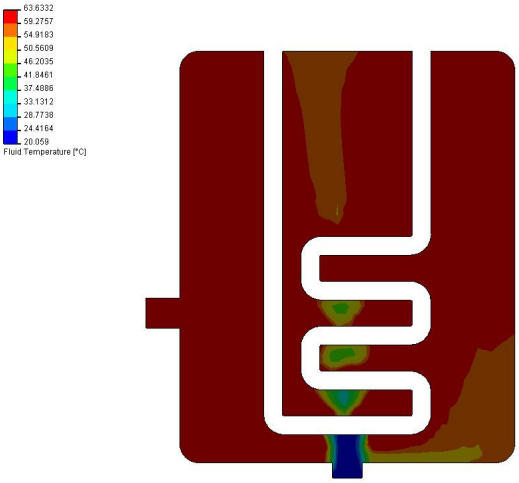

(b) fluid temperature through lateral vertical section.

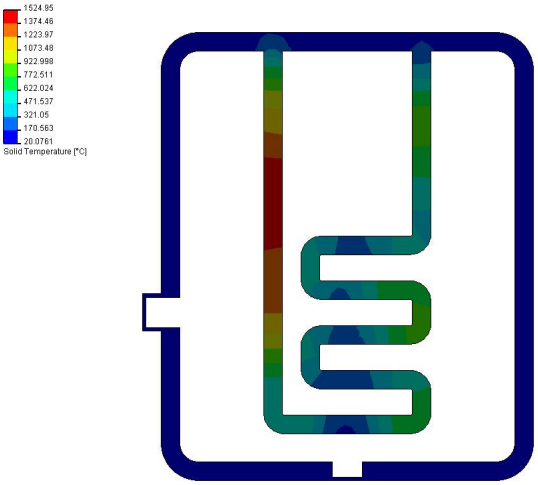

(c) solid temperature through front lateral section.
Fig. 19. Distribution of temperature for case no.4

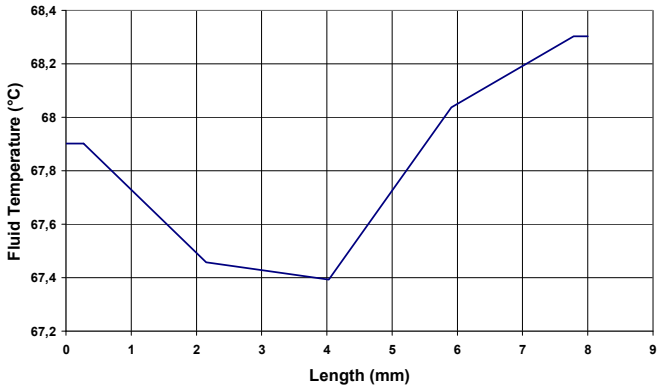

Fig. 13. Variation of water temperature on the outlet for case no.4.

4 Solution optimization

There are some evident flaws that have been determined by numerical simulation of electric heaters. Therefore a separate study has been pursued to determine an optimized solution.

In this respect a new simulation has been conceived for a new form of helical electric heater, currently used for other applications. The analysis has been made for both lateral and bottom position of water inlet.

The general appearance of the modified model is presented in figure 20.

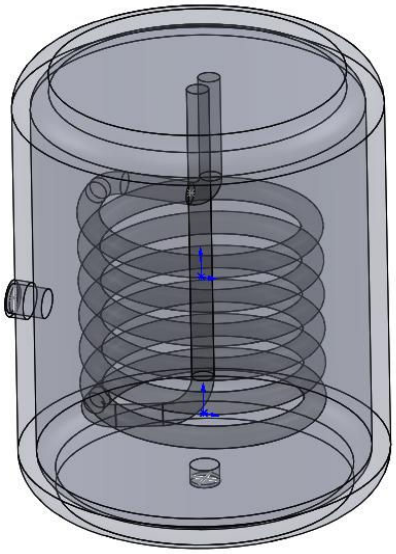

Fig. 20. General appearance of the modified three-dimensional model.

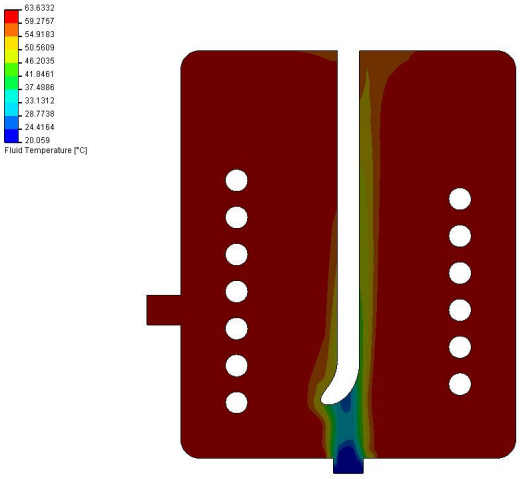

(a) fluid temperature through front vertical section.

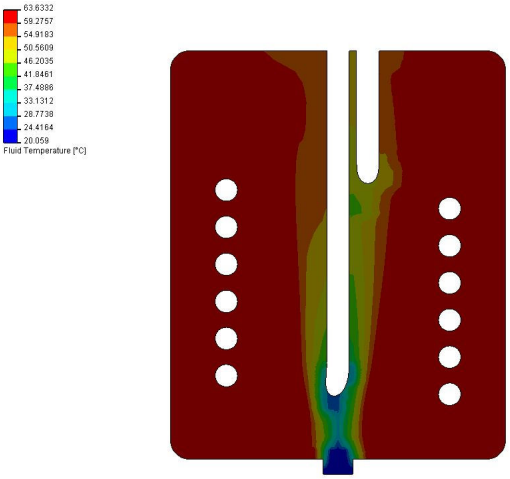

(b) fluid temperature through lateral vertical section.

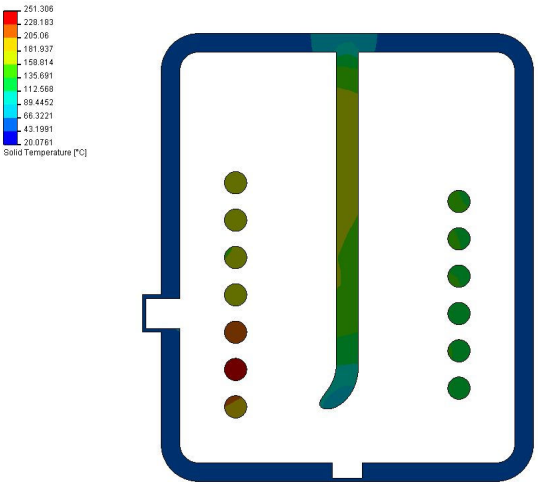

(c) solid temperature through front vertical section.
Fig. 21. Distribution of temperature for bottom inlet of water.

An analysis of the temperature distribution of fluid inside container (figure 21 a, b) reveals that difference between maximum and minimum level is significantly smaller, without any isolated area where water is very hot.
The most important benefit of the new solution consists in the maximum temperature of the heating element, which is considerable lower in comparison with the classic solution, i.e. under 300°C. This would probably reduce considerably the thermal load and increase durability.
The outlet temperature is much more favorable (figure 22), with a range at the very middle of the required values.

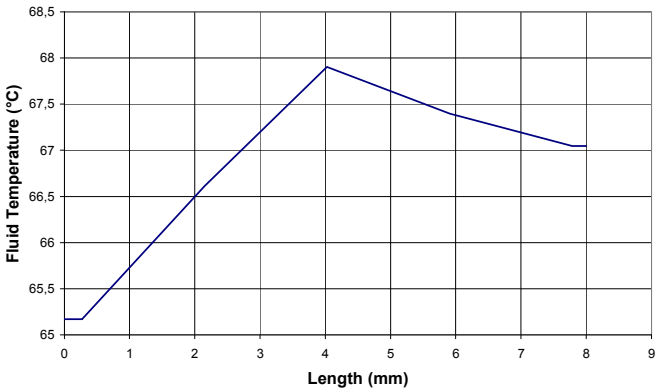

Fig. 22. Variation of water temperature on the lateral water outlet.

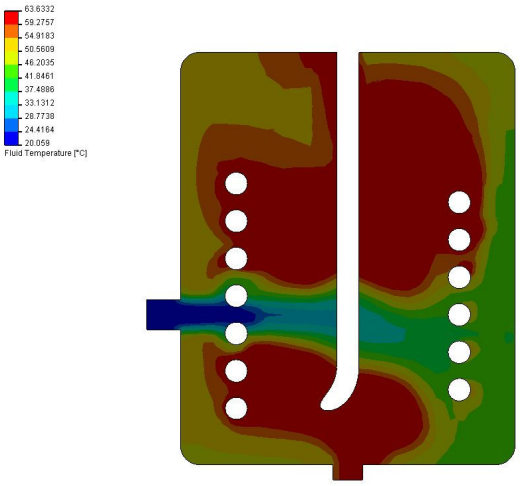

(a) fluid temperature through front vertical section.

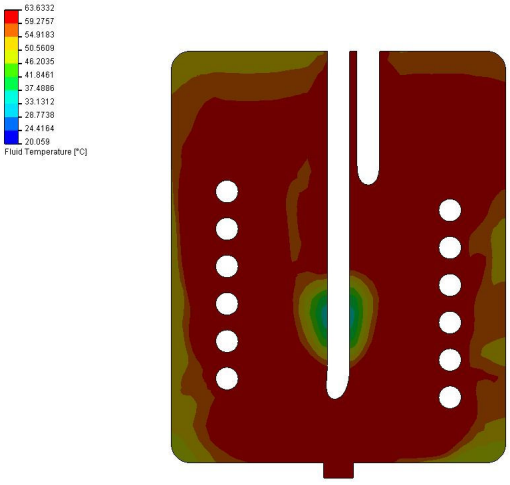

(b) fluid temperature through lateral vertical section.

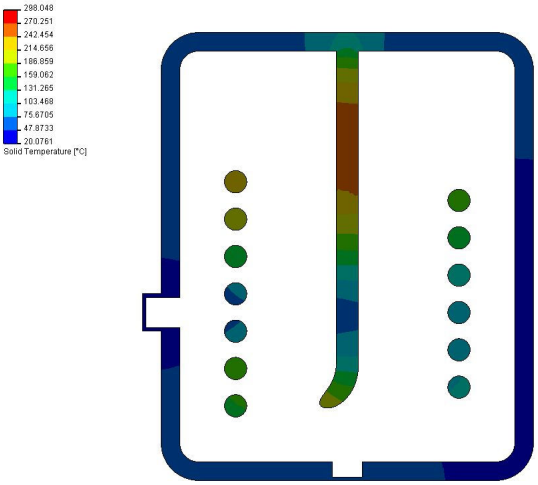

(c) solid temperature through front vertical section.
Fig. 23. Distribution of temperature for lateral inlet of water.

Similar results have been obtained if water is introduced through bottom orifice (figure 23). The temperature of outlet water is somehow lower and the distribution is less favorable (figure 24).

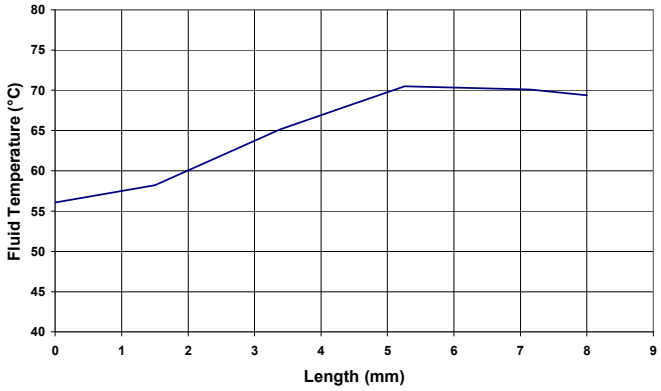

Fig. 24. Variation of water temperature on the bottom water outlet.

4 Conclusions

Numerical analysis of fluid flowing and heat transfer for an existing water heater revealed that temperature of electric heater is close to the maximum acceptable values of 900°C. The temperature of warm water is conforming to general requirements, but volumes of fluid with maximum temperature stagnate inside container. Simple constructive solutions, such as modification of position for heating element or reversing inlet and outlet orifices do not improve flowing and heat transfer.

The new solution based on a helical heating element could be of significant benefit, since distribution of fluid temperature is more uniform and favorable. The most important improvement consists in more reduced loading of the heating element, which has a much lower maximum temperature, under 300°C, is more likely to improve durability.

References:

[1] European Environment Agency, *Greenhouse gas emission trends and projections in Europe 2009 - Tracking progress towards Kyoto targets*, EEA Report No 9/2009.

[2] W. S. Janna, *Engineering heat transfer,* CRC Press, Boca Raton, London New York, Washington, D.C.2000

[3] S. S. Rao, *The Finite Element Method in Engineering*, Elsevier Butterworth–Heinemann, 2005.

[4] T. Tanaka, *Fundamental Study on Energy Transfer Mechanism Caused in Turbomachinery*, WSEAS TRANSACTIONS on FLUID MECHANICS, Issue 6, Volume 1, June 2006, pp. 550-557

[5] F.-K. Benra, *Fluid-Structure-Interaction: Fundamentals and Engineering Applications,* 2nd WSEAS International Conference on APPLIED AND THEORETICAL MECHANICS (MECHANICS '06), Venice, Italy, November 20-22, 2006

[6] D. Dobersek, D. Goricanec, *Evaluation of Thermal Flow Losses and Increased Consumption of Electricity due to Water Scale Precipitation on Heaters of Domestic Appliances*, 5th WSEAS Int. Conf. on Heat and Mass transfer (HMT'08) , Acapulco, Mexico, January 25-27, 2008, pp. 127-131

[7] A. S. Hanafi, H.F. Elbakhshawangy, *Numerical Determination of Temperature and Velocity Profiles for Forced and Mixed Convection Flow through Narrow Vertical Rectangular Channels*, 5th WSEAS Int. Conf. on Heat and Mass transfer (HMT'08) , Acapulco, Mexico, January 25-27, 2008, pp. 132-139

[8] W. S. Janna, *Engineering Heat Transfer*, Second Edition, CRC Press Boca Raton London New York Washington, D.C., 2000